A R C H I V E S O F M E T A L L U R G Y A N D M A T E R I A L S
Volume 50 2005 Issue 4

W. WOŁCZYŃSKI*, J. JANCZAK-RUSCH**, J. KLOCH*** , T. RÜTTI**, T. OKANE****

A MODEL FOR SOLIDIFICATION OF INTERMETALLIC PHASES FROM Ni-Al SYSTEM AND ITS APPLICATION TO DIFFUSION SOLDERING

MODEL KRYSTALIZACJI FAZ MIĘDZYMETALICZNYCH Z UKŁADU Ni-Al I JEGO ZASTOSOWANIE DO SPAJANIA DYFUZYJNEGO

The physical limitations of the back-diffusion parameter for the formation of solid solution in the *Bridgman* system are discussed and referred to a schematically drawn equilibrium phase diagram. The back-diffusion parameter is employed to develop the model for redistribution to its new version describing the formation of intermetallic phases resulting from the peritectic reactions. Solute redistribution and thickness of sub-layers are measured in soldered Ni-Al-Ni interconnections. The confrontation of the solute redistribution profile predicted by the model and solute redistribution profile measured in the interconnections suggests that the model can be applied to reproduce both experimental redistribution and ratio of solidified sub-layers by the theoretical predictions. The effect of the back-diffusion onto thickening of sub-layers and solute redistribution in the Ni-Al-Ni interconnection is discussed.

Analizuje się fizykalne ograniczenia parametru dyfuzji wstecznej dla formowania się pojedynczej fazy stałej w systemie *Bridgman'a*. Analiza odniesiona jest do diagramu fazowego. Parametr dyfuzji wstecznej wykorzystano do opracowania zmodyfikowanej wersji modelu redystrybucji opisującej powstawanie faz międzymetalicznych jako wynik reakcji perytektycznych. Redystrybucja składnika oraz szerokość warstewek zostały zmierzone w spajanym dyfuzyjnie złączu Ni-Al-Ni. Zestawienie profilu redystrybucji składnika przewidzianego modelem ze zmierzonym profilem redystrybucji składnika wskazuje że model może być zastosowany celem teoretycznego odtworzenia zarówno redystrybucji eksperymentalnej jak też proporcji krzepnących warstewek. Dyskutuje się wpływ dyfuzji wstecznej na pogrubianie się warstewek i na redystrybucję składnika w złączu Ni-Al-Ni.

* INSTYTUT METALURGII I INŻYNIERII MATERIAŁOWEJ IM. A. KRUPKOWSKIEGO, PAN, 30-059 KRAKÓW, UL. REYMONTA 25

** LABORATORY OF JOINING AND INTERFACE TECHNOLOGY, SWISS FEDERAL LABORATORIES FOR MATERIALS TESTING AND RESEARCH EMPA, 8600 DÜBENDORF, ÜBERLAND ST. 129, SWITZERLAND

*** INSTYTUT MATEMATYKI, POLSKA AKADEMIA NAUK, 31- 027 KRAKÓW, UL. ŚW. TOMASZA 30

**** THE NATIONAL INSTITUTE OF ADVANCED INDUSTRIAL SCIENCE AND TECHNOLOGY AIST, TSUKUBA EAST, 1-2 NAMIKI, IBARAKI 305 8564, JAPAN

Notation

D	diffusion coefficient in the solid, [$\mu m^2/s$]
k	partition ratio, [mole fr./mole fr.]
L^0	initial amount of the liquid, $L^0 = 1$, dimensionless
N	solute concentration, [mole fr.]
N^B	solute redistribution in the solid, [mole fr.]
N^D	solute secondary redistribution in the solid (diffusive shift) required by the peritectic reaction, [mole fr.]
N^E	solute concentration at the eutectic point on the phase diagram, [mole fr.]
N^F	solute concentration at the intersection of the temperature, T_R and *liquidus* line of a given phase diagram, [mole fr.]
N^L	solute concentration in liquid, [mole fr.]
N^S	solute microsegregation at the s/l interface (historical solute concentration) [mole fr.]
N_i^D	solute secondary redistribution in the solid (diffusive shift), required by the i — peritectic reaction, [mole fr.]
N_i^L	solute concentration in the liquid for i - ranges of solidification, [mole fr.]
N_i^S	solute microsegregation at the solid/liquid interface (historical solute concentration), [mole fr.]
N_i^{DP}	reproduced solute redistribution due to the current model to confront it with the experimental solute redistribution, [mole fr.]
N_i	characteristic points on *liquidus* line of a given phase diagram showing the solute concentration adequate for a given peritectic reaction, $N_i = N_1$, N_2 [mole fr.]
N_0	initial concentration of the solute for solidification; also, average solute content within both sub-layers formed during diffusion soldering, [mole fr.]
N_1	solute concentration in the liquid (phase diagram) at first peritectic reaction, [mole fr.]
N_2	solute concentration in the liquid (phase diagram) at second peritectic reaction, [mole fr.]
t	current local solidification time, $t \in \left[0, t^F\right]$, [s]
t^F	total local solidification time for solidification and precipitation, [s] or local solidification time for solidification completed during diffusion soldering (Fig. 10), [s]
t^K	local solidification time for solid/precipitate boundary formation, [s] or local solidification time for solidification arrested during diffusion soldering (Fig. 10), [s]
t^0	local solidification time representing the freezing, [s]
T	temperature, [K]

T_R temperature at which diffusion soldering occurs, [K]

x current amount of the growing solid, $x \in [0,1]$, dimensionless $x_1^{\max}$ is equal to $x_i^{\max}$ for $i = 1$

$x_i^{\max} - x_i^{\min}$ amount of peritectic phase for a given i - solidification range, dimensionless

X^F amount of the growing sub-layers for solidification completed during diffusion soldering (Fig. 10), dimensionless

X^K amount of the growing solid at the boundary solid/precipitate, dimensionless or amount of the growing sub-layers for solidification arrested during diffusion soldering (Fig. 10), dimensionless

X^0 amount of the solid for frozen solidification, dimensionless or amount of the solid for solidification arrested during diffusion soldering, $X^0 = X^K = 1$, for each arrested multi-layer, (Fig. 10), dimensionless

α^D parameter of back-diffusion for solute redistribution, dimensionless

α_i^D parameter of back-diffusion for solute redistribution, i - number of solidification ranges, dimensionless

α_i^P parameter of back-diffusion for peritectic reaction, i - number of peritectic reactions, dimensionless

β^{ex} coefficient of the extension of solute redistribution, dimensionless

β^{in} coefficient of the intensity of solute redistribution, dimensionless

γ distance, [μm]

γ^F distance from the centre of cell to the boundary cell/cell or intercellular spacing for an cellular array, [μm]

γ^K distance from the centre of cell to the boundary solid/precipitate, [μm]

γ^0 distance from the centre of cell to the frozen solid/liquid interface, [μm]

λ_1^F thickness of the first sub-layer for solidification completed during diffusion soldering (Fig. 10), [μm]

γ_2^F thickness of the second sub-layer for solidification completed during diffusion soldering, (Fig. 10), [μm]

γ_1^K thickness of the first sub-layer for solidification arrested during diffusion soldering (Fig. 10), [μm]

γ_2^K thickness of the second sub-layer for solidification arrested during diffusion soldering (Fig. 10), [μm]

1. Solute redistribution for the solid solution formation in the *Bridgman* system

The Scheil's theory [1] for 3D dendritic microsegregation/redistribution was firstly adapted by B r o d y and F l e m i n g s [2] to 2D directional growth with introducing the back-diffusion phenomenon. In the case of 2D growth (*Bridgman* system) the definition of back-diffusion parameter $\alpha^D = const.$, for cellular growth, Fig. 1, is:

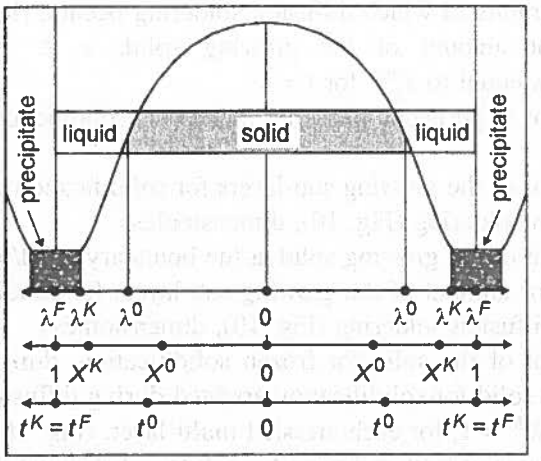

Fig. 1. Frozen cellular / dentrtic morphology showing schematically geometrical profile of the solid/liquid (s/l) interface, related to 2D solidification; s/l volume element defines the parameters resulting from freezing

$$\alpha^D = Dt^0\left(\lambda^0\right)^{-2} \qquad \lambda^0 \in \left[0, \lambda^K\right] \qquad t^0 \in \left[0, t^K\right]. \tag{1}$$

The α^D — parameter plays essential role in prediction of cellular microsegregation [3]. Microsegregation is defined by the following equation describing the behaviour of the formerly (historically) existing solid/liquid interfaces.

$$N^S(x;\alpha^D, L^0, N_0, k) = kN_0\left[\left(L^0 + \alpha^D kx - x\right)\Big/L^0\right]^{(k-1)/(1-\alpha^D k)} \qquad x \in \left[0, X^K\right] \tag{2}$$

with

$$N^L(x;\alpha^D, L^0, N_0, k) = N_0\left[\left(L^0 + \alpha^D kx - x\right)\Big/L^0\right]^{(k-1)/(1-\alpha^D k)}. \tag{2a}$$

The solute redistribution superposes on the microsegregation, eqn. (2), and is given:

$$\begin{aligned} N^B(x;X^0,\alpha^D, L^0, N_0, k) &= [\ 1 + \beta^{ex}(x;X^0, L^0, k)\beta^{in}(X^0,\alpha^D, L^0, k)\ ] \\ N^S\left(x;\alpha^D, L^0, N_0, k\right) &\quad x \in \left[0, X^0\right] \quad X^0 \in \left[0, X^K\right], \end{aligned} \tag{3}$$

where, the coefficients of redistribution intensity β^{in} and redistribution extent β^{ex} are given, respectively

$$\beta^{in}(X^0,\alpha^D,L^0,k)=\{\,\alpha^D(2\alpha^D k-k-1)\,[\,(L^0+kX^0-X^0)N^L(X^0,\alpha^D,L^0,1,k)-L^0\,]\times (L^0+kX^0-X^0)\,\}\times\{\,(k-1)\,[\,(L^0)^2N^L(X^0,\alpha^D,L^0,1,k)-(L^0)^2+ X^0L^0\,(\,2(\alpha^D k-1)N^L(X^0,\alpha^D,L^0,1,k)-2\alpha^D k+k+1\,)+ (\,\alpha^D kX^0-X^0\,)^2\,N^L(X^0,\alpha^D,L^0,1,k)\,]\,\}^{-1} \tag{4}$$

$$\beta^{ex}(x;X^0,L^0,k)=\frac{(1-k)(X^0-x)}{L^0+kX^0-X^0}. \tag{5}$$

The back-diffusion parameter α^D, eqn. (1) operates in such a way that hypothetical localization of the solid/liquid interface, $N^S(X^0;0,L^0,N_0,k)$ resulting from the Scheil's model [1] is translated to the new position $N^S(X^0;\alpha^D,L^0,N_0,k)$, Fig. 2, [4].

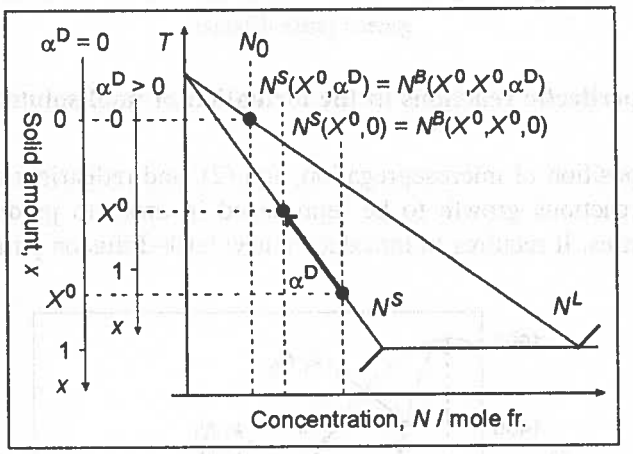

Fig. 2. Physical meaning of the α^D back-diffusion parameter in solidification shown for an arbitrary phase diagram

The solute redistribution coefficient defined as a product of extension and intensity of the solute redistribution $\beta(x;X^0,\alpha^D,L^0,k) = \beta^{ex}(x;X^0,L^0,k)\beta^{in}(X^0,\alpha^D,L^0,k)$ is responsible for a shift of *solidus* line as it is shown schematically in Fig. 3. The coefficient is effected by the back diffusion parameter, α^D.

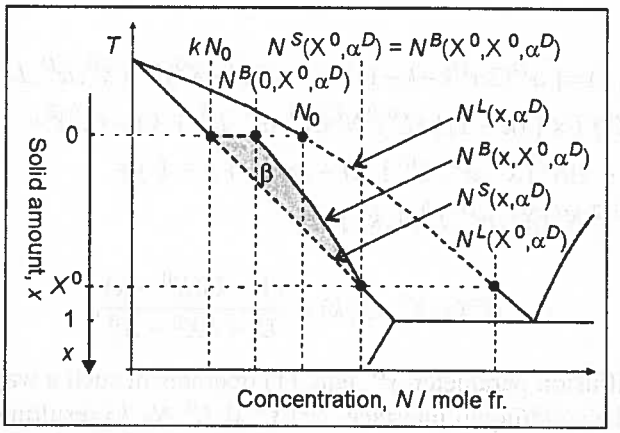

Fig. 3. Physical meaning of the $\beta(x; X^0, \alpha^D, L^0, k)$ solute redistribution coefficient illustrated for a general phase diagram

2. Role of peritectic reactions in the formation of final solute redistribution

The superposition of microsegregation, eqn (2), and redistribution eqn. (3) allows the peritectic reactions growth to be reproduced in order to predict the amount of two formed phases. It requires to introduce a new back-diffusion parameter, α_i^P, which

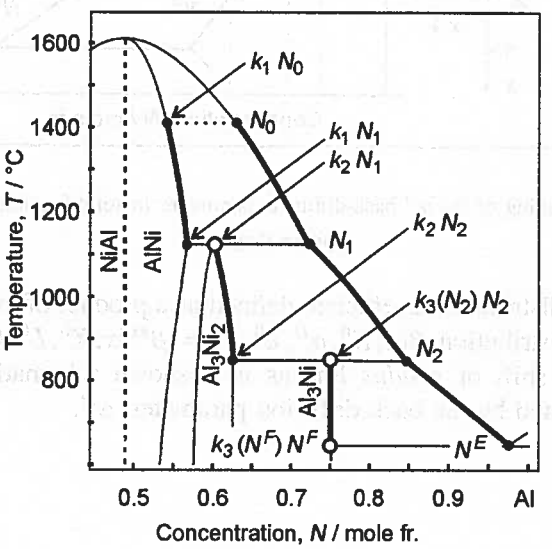

Fig. 4. Solidification path $N_0 \div N_1 \div N_2 \div N^E$, and historical s/l interface path: $k_1N_0 \div k_1N_1 \div k_2N_1 \div k_2N_2 \div k_3N - 2$ referred to two peritectic reactions according which intermetallic phase Al_3Ni_2 and intermetallic compound Al_3Ni are formed during non-equilibrium solidification

decides (together with solidification path, Fig. 4) on a thickening of two phases: Al_3Ni_2 — intermetallic phase and Al_3Ni — intermetallic compound (in the case of Ni-Al system), $i = 1,...n$; $n = 2$.

$$\alpha_i^P = D_i t^K \left(\lambda_i^K\right)^{-2}. \tag{6}$$

Solidification involves two peritectic reactions: 1/ $AlNi + liquid(N_1) \Rightarrow Al_3Ni_2$, and 2/ $Al_3Ni_2 + liquid(N_2) \Rightarrow Al_3Ni$, in sequence. As a result two mentioned intermetallic phase/compound are formed, as illustrated in Fig. 4. The reactions modify the solute redistribution profile. According to the present model the final redistribution is representing by a plane concentration profile resulting from the localization of the peritectic reaction in the Ni-Al phase diagram: k_2N_1 and k_3N_2, Fig. 4.

However, eqn. (2) and eqn. (3) are to be developed because two ranges of solidification exist (while considering simplified solidification path): $N_0 \div N_1$, $N_1 \div N_2$, along which mentioned intermetallic phase Al_3Ni_2 and intermetallic compound Al_3Ni, are formed ($n = 2$). Therefore, three solidification ranges are to be considered while considering full solidification path: $N_0 \div N_1$, $N_1 \div N_2$, $N_2 \div N^F$; ($n = 3$).

It requires to introduce some additional formulas related to each solidification range resulting from the phase diagram, Fig. 4 (with the number of solidification ranges $n = 2$ or $n = 3$ in the case of the formation of intermetallic phase Al_3Ni_2 and intermetallic compound Al_3Ni known from the Ni-Al phase diagram):

$$l_i^0 = \begin{cases} L^0, i = 1; \\ L^0 - x_1^{\max} i = 2 \end{cases} \qquad x_i^0 = \begin{cases} X^0, i = 1; \\ X^0 - x_1^{\max} i = 2. \end{cases} \tag{6a}$$

Actually, eqn. (2) is transformed into:

$$N_i^S(x; \alpha_i^D, l_i^0, N_{i-1}, k_i) = k_i N_{i-1} \left[\left(l_i^0 + \alpha_i^D k_i x - x\right)/l_i^0\right]^{(k_i-1)/(1-\alpha_i^D k_i)} \quad i = 1,2 \tag{7}$$

because n — ranges of solidification are considered, where the behaviour of the liquid along the solidification path is described by the eqn. (2a) transformed into:

$$N_i^L(x; \alpha_i^D, l_i^0, N_{i-1}, k_i) = N_{i-1} \left[\left(l_i^0 + \alpha_i^D k_i x - x\right)/l_i^0\right]^{(k_i-1)/(1-\alpha_i^D k_i)}. \tag{8}$$

The developed eqn. (7) and eqn (8) depend on number of solidification ranges resulting from solidification path while eqn. (2) and eqn. (2a) are delivered for the growth of one solid solution, only.

Analogously, eqn. (9) is given by eqn. (3) for $X^0 = x_i^0$ and $L^0 = l_i^0$:

$$\begin{aligned} &N_i^B(x; x_i^0, \alpha_i^D, l_i^0, N_{i-1}, k_i) = \\ &[\,1 + \beta_i^{ex}(x; x_i^0, l_i^0, k_i)\beta_i^{in}(x_i^0, \alpha_i^D, l_i^0, k_i)\,]\, N_i^S\left(x; \alpha_i^D, l_i^0, N_{i-1}, k_i\right), \end{aligned} \tag{9}$$

where the coefficient of the extent of solute redistribution is modified due to eqn. (5):

$$\beta_i^{ex}\left(x; x_i^0, l_i^0, k_i\right) = \frac{(1-k_i)(x_i^0 - x)}{(l_i^0 + k_i x_i^0 - x_i^0)} \tag{10}$$

with the coefficient of the intensity of solute redistribution defined due to eqn. (4):

$$\begin{aligned}
&\beta_i^{in}(x_i^0, \alpha_i^D, l_i^0, k_i) = \\
&\{\, \alpha_i^D(2\alpha_i^D k_i - k_i - 1)\,[\,(l_i^0 + k_i x_i^0 - x_i^0) N_i^L(x_i^0, \alpha_i^D, l_i^0, N_{i-1}, k_i) - l_i^0\,]\times \\
&(l_i^0 + k_i x_i^0 - x_i^0)\,\} \times \{\,(k_i - 1)\,[\,\left(l_i^0\right)^2 N_i^L(x_i^0, \alpha_i^D, l_i^0, N_{i-1}, k_i) - \left(l_i^0\right)^2 + \\
&x_i^0 l_i^0\,(\,2(\alpha_i^D k_i - 1) N_i^L(x_i^0, \alpha_i^D, l_i^0, N_{i-1}, k_i) - 2\alpha_i^D k_i + k_i + 1\,) + \\
&(\,\alpha_i^D k_i x_i^0 - x_i^0\,)^2 N_i^L(x_i^0, \alpha_i^D, l_i^0, N_{i-1}, k_i)\,]\,\}^{-1}\,.
\end{aligned} \tag{11}$$

A peritectic reactions involve new solute concentration (secondary redistribution), N_i^D within primary phases AlNi and Al_3Ni_2. It is reproduced in the current model as a diffusive shift N_i^D of the primary redistribution N_i^B.

$$N_i^D(x; x_i^0, \alpha_i^D, \alpha_i^P, l_i^0, N_{i-1}, N_i, k_i, k_{i+1}) = N_i^B(x + x_i - x_i^{min}; x_i, \alpha_i^D, l_i^0, N_{i-1}, k_i). \tag{12}$$

The amount of x_i — primary phases formed in each of solidification range is given by eqn. (8) for

$$N_i^L\left(x_i; \alpha_i^D, l_i^0, N_{i-1}, k_i\right) = N_i \tag{13}$$

by

$$x_i(\alpha_i^D, l_i^0, N_{i-1}, N_i, k_i) = l_i^0\,[\,1 - \alpha_i^D k_i\,]^{-1}\,[\,1 - (N_i/N_{i-1})^{(1-\alpha_i^D k_i)/(k_i-1)}\,]\,. \tag{14}$$

The formation sequence of peritectic phases (first the formation of the Al_3Ni_2 intermetallic phase and next the formation of intermetallic compound Al_3Ni) are simulated for solidification process in two steps.
At first, x_i^{max} parameter is defined according to a given phase diagram:

$$\begin{aligned}
&x_i^{max}(x_i^0, \alpha_i^D, \alpha_i^P, l_i^0, N_{i-1}, N_i, k_i, k_{i+1}) = x_i^{mem}(x_i^0, \alpha_i^D, \alpha_i^P, l_i^0, N_{i-1}, N_i, k_i, k_{i+1}); \\
&\text{when} r_i(\alpha_i^D, l_i^0, N_{i-1}, N_i, k_i, k_{i+1}) > (N_i - k_{i+1} N_i)\times \\
&[\, x_i^{mem}(x_i^0, \alpha_i^D, \alpha_i^P, l_i^0, N_{i-1}, N_i, k_i, k_{i+1}) - x_i(\alpha_i^D, l_i^0, N_{i-1}, N_i, k_i)\,]
\end{aligned} \tag{15}$$

or

$$
\begin{aligned}
&x_i^{max}(x_i^0, \alpha_i^D, \alpha_i^P, l_i^0, N_{i-1}, N_i, k_i, k_{i+1}) = x_i(\alpha_i^D, l_i^0, N_{i-1}, N_i, k_i) + \\
&r_i(\alpha_i^D, l_i^0, N_{i-1}, N_i, k_i, k_{i+1}) \Big/ (N_i - k_{i+1}N_i); \\
&when r_i(\alpha_i^D, l_i^0, N_{i-1}, N_i, k_i, k_{i+1}) \leqslant (N_i - k_{i+1}N_i) \times \\
&[\, x_i^{mem}(x_i^0, \alpha_i^D, \alpha_i^P, l_i^0, N_{i-1}, N_i, k_i, k_{i+1}) - x_i(\alpha_i^D, l_i^0, N_{i-1}, N_i, k_i) \,]
\end{aligned}
\tag{16}
$$

$$
\begin{aligned}
&r_i(\alpha_i^D, l_i^0, N_{i-1}, N_i, k_i, k_{i+1}) = \\
&k_{i+1}N_i x_i(\alpha_i^D, l_i^0, N_{i-1}, N_i, k_i) - \int_0^{x_i} N_i^B(x; x_i, \alpha_i^D, l_i^0, N_{i-1}, k_i)dx
\end{aligned}
\tag{16a}
$$

$$
\begin{aligned}
&x_i^{mem}(x_i^0, \alpha_i^D, \alpha_i^P, l_i^0, N_{i-1}, N_i, k_i, k_{i+1}) = \min\left\{x_i^0;\, x_i(\alpha_i^D, l_i^0, N_{i-1}, N_i, k_i) + \right. \\
&[\, x_i(\alpha_i^P, l_i^0, k_{i+1}N_i, N_i, k_{i+1}) - x_i(\alpha_i^P, l_i^0, k_{i+1}N_i, N_i, k_i) \,] \times \\
&[\, x_i(\alpha_i^P, l_i^0, k_{i+1}N_i, N_i, k_i) - x_i(0, l_i^0, k_{i+1}N_i, N_i, k_i) \,] \times \\
&\left.[\, x_i(1, l_i^0, k_{i+1}N_i, N_i, k_i) - x_i(0, l_i^0, k_{i+1}N_i, N_i, k_i) \,]^{-1} \right\}.
\end{aligned}
\tag{16b}
$$

The $x_i\,(\alpha_i^D, l_i^0, N_{i-1}, N_i, k_i)$ parameter used in eqn. (15) and eqn. (16) is generally given by eqn. (14). Next $x_i^{\min}$ — parameters is determined from the mass balance:

$$
\begin{aligned}
&\int_0^{x_i^{min}} [\, N_i^B(x + x_i - x_i^{min}; x_i, \alpha_i^D, l_i^0, N_{i-1}, k_i) - N_i^B(x; x_i, \alpha_i^D, l_i^0, N_{i-1}, k_i) \,]\, dx + \\
&\int_{x_i^{min}}^{x_i} [\, k_{i+1}N_i - N_i^B(x; x_i, \alpha_i^D, l_i^0, N_{i-1}, k_i) \,]\, dx = \\
&(N_i - k_{i+1}N_i)\,[\, x_i^{\max}(x_i^0, \alpha_i^D, \alpha_i^P, l_i^0, N_{i-1}, N_i, k_i, k_{i+1}) - x_i(\alpha_i^D, l_i^0, N_{i-1}, N_i, k_i)].
\end{aligned}
\tag{17}
$$

The final profile of the Al-solute redistribution with the ratio of the amount of both intermetallic phase and compound calculated due to eqns (6)-(17) is shown in Fig. 5. The profile of primary redistribution of solute, eqn. (9), within primary phases AlNi and Al_3Ni_2 is marked by dashed line, Fig. 5.

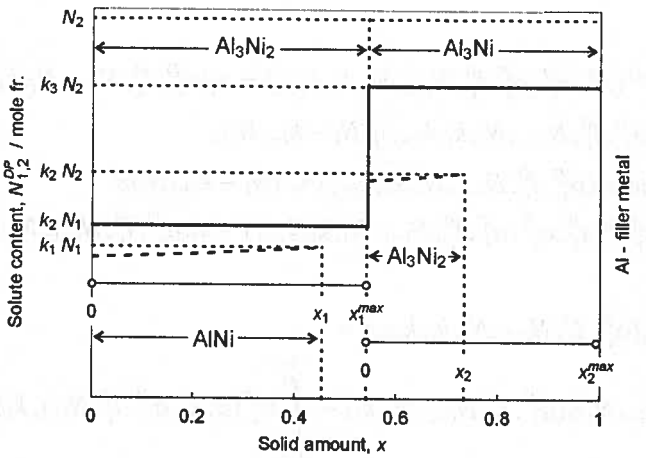

Fig. 5. Reproduction of the final Al-solute redistribution and ratio of both intermetallic phase and compund after two peritectic reactions due to the simplified solidification path $N_0 \div N_1 \div N_2$, as defined in Fig. 4

3. Experimental Al — solute redistribution within the Ni/Al/Ni interconnection

The analysed Ni-Al-Ni interconnections were produced in a specially designed apparatus for diffusion soldering/brazing under vacuum applying isothermal solidification, defined by the temperature, T_R, Fig. 6. The constructed apparatus allows a solidification

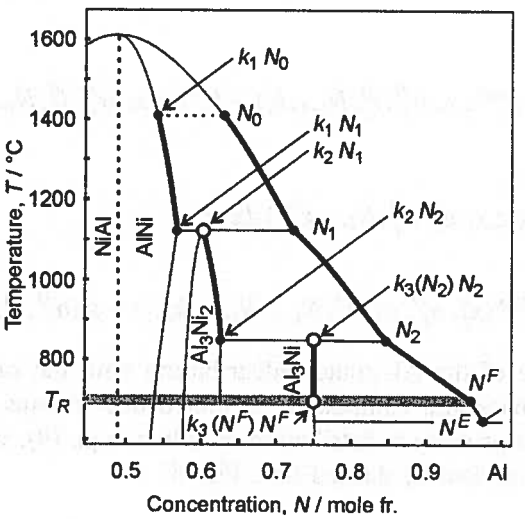

Fig. 6. Solidification path within the Ni-Al phase diagram: $N_0 \div N_1 \div N_2 \div N^F$, and historical s/l interface path: $k_1N_0 \div k_1N_1 \div k_2N_1 \div k_2N_2 \div k_3N_2$ as referred to the formation of soldered interconnection Ni/Al/Ni at T_R = 700°C

process to be arrested after a predetermined time. An arresting is efficient due to the injection of an inert gas into the vacuum chamber in which sample is placed. The period of time, t^K, from beginning of solidification to the applied freezing is introduced into the definition of the back-diffusion parameter, eqn. (6), under assumption that both sub-layers solidified simultaneously.

Many samples were produced with application of different time of freezing in order to estimate average Al-solute concentration within the sub-layers, N_0. It has been found that $N_0 \cong 0.66$ [mole fr.]. The arrested morphology together with Al-solute redistribution are shown in Fig. 7. It seems evident that the predicted profile of redistribution shown in Fig. 5 can fit the measured profile, Fig. 7, with good accuracy. The suggested confrontation of both profiles is shown in Fig. 8.

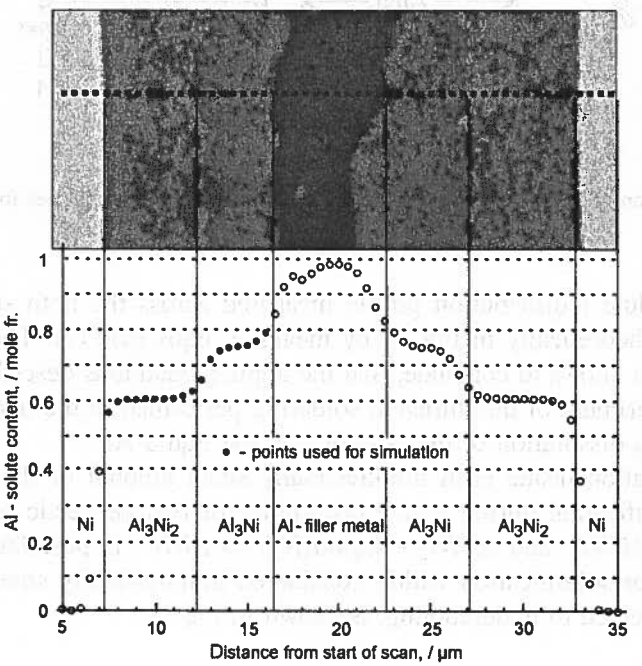

Fig. 7. Sequence of peritectic phases within the Ni/Al/Ni interconnection. Solidification arrested after 121 seconds of the isothermal solidification at T_R = 700°C; EDS analysis of the Al-solute redistribution across the interconnection

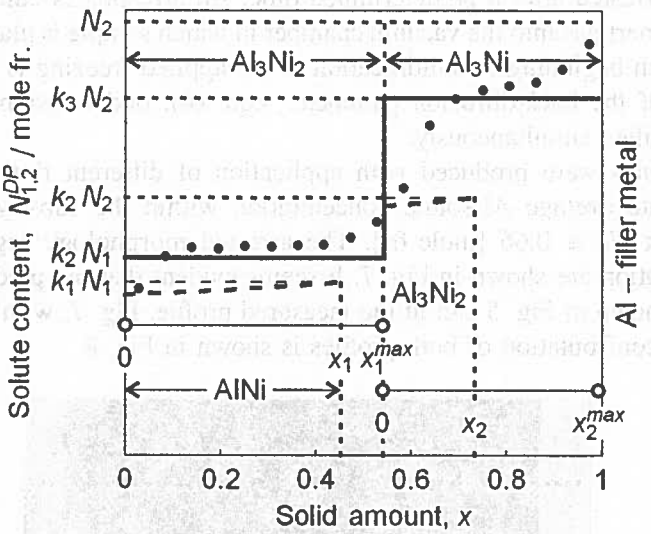

Fig. 8. Reproduction of Al-solute redistribution and thickness of peritectic phases for soldered Ni-Al-Ni multi-layer interconnection

The Al–solute redistribution profile measured across the both sub-layers, Fig. 7 is reproduced theoretically in Fig. 8, by means of eqns (6)-(17). The good accuracy of confrontation allows to conclude, that the applied equations describe adequately an isothermal experiment of the diffusion soldering performed in the under-cooled liquid formed due to a dissolution of the Ni-atoms in the liquid Al.

The dissolution inside each infinitesimally small amount of the liquid, dx, precedes the solidification during which occurrence of two peritectic reactions: $AlNi + liquid(N_1) \Rightarrow Al_3Ni_2$, and $Al_3Ni_2 + liquid(N_2) \Rightarrow Al_3Ni$, is postulated, [5]. The operating range for solidification within considered infinitesimally small amount of the liquid, dx, subjected to undercooling, is shown in Fig. 9.

4. Concluding remarks

The simple model for 2D solute redistribution, eqns (1)-(5) connected with formation of one solid solution by means of the *Bridgman* system has been developed to more complicated approach, eqns (6)-(17) describing the formation sequence of intermetallic phases and compounds during peritectic reactions. The approach is referred to Ni-Al phase diagram according which Al_3Ni_2 intermetallic phase and Al_3Ni intermetallic compound are formed in sequence.

The calculated Al-solute redistribution profile and thicknesses of intermetallic phase and compound, Fig. 5, are subjected to the confrontation, Fig. 8, with experimental profile of Al-solute redistribution and thicknesses of two sub-layers, Fig. 7,

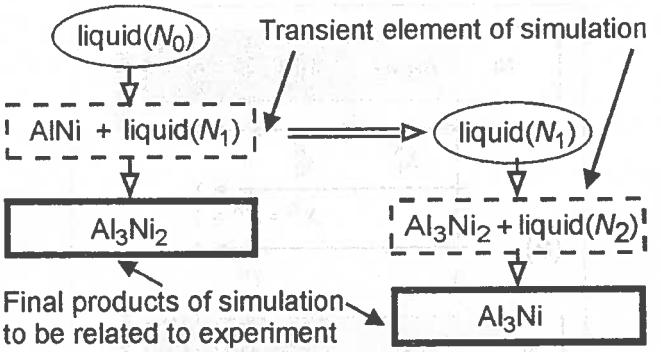

Fig. 9. Operating range for the undercooled peritectic reactions within infinitesimally small amount of the Al-liquid, dx, containing dissolute Ni-atoms and involving two peritectic reactions in sequence

obtained by the diffusion soldering arrested during solidification (disappearance of the Al liquid filler metal).

A good agreement between theoretical profile and experimental profile is obtained, Fig. 8. Therefore, it can be concluded that applied mode of calculation, eqns (6)-(17) is appropriate to characterize the sequential formation of intermetallic phases and compounds during diffusion soldering.

In current analysis no precipitates (liquid — N^F) are considered due to the assumed simplified solidification path, $N_0 \div N_1 \div N_2$, Fig. 4 or Fig. 6. The assumption is confirmed by satisfactory fitting of experimental points, Fig. 8, however solidification path elongated to the N^F — point on *liquidus* line, Fig. 6 should also be envisaged.

The back-diffusion parameter α^D depends on local solidification time, t^0, eqn. (1). In the case of soldered multi-layer interconnections the definition of the α_i^D and α_i^P parameters are referred to the time of arresting, t^K, applied to experiment in order to stopped the sequential growth of both peritectic phases: Al_3Ni_2 and Al_3Ni, Fig. 10.

Generally, $0 \leqslant \alpha i^D \leqslant 1$; $0 \leqslant \alpha i^P \leqslant 1$; but $\alpha i^D = 0$, $\alpha i^P = 0$ for the non-diffusive growth, according to the Scheil's model [1], and $\alpha i^D = 1$, $\alpha i^P = 1$ for the equilibrium solidification, [4]. The value of back-diffusion parameter can be assumed due to above inequalities, but applying an optimization procedure (fitting of the experimental redistribution [3]).

The α^D back-diffusion parameter initially defined for 2D growth, eqn. (1), is actually introduced as α_i^D and α_i^P, into the model, to describe a thickening of soldered multi-layer interconnections, Fig. 10. The physical meaning of the α^D back-diffusion parameter is explained on the basis of phase diagram, Fig. 2, and its effect on redistribution in Fig. 3.

Thus, $\beta^{in}(X^0, 0, L^0, k) = 0$; $\beta = \beta^{ex}(x, X^0, L^0, k)\beta^{in}(X^0, 0, L^0, k) = 0$ (for non-diffusive solidification described as by the Scheil model [1]), $\beta^{in}\left(X^0, 1, L^0, k\right) = 1$;

$\beta = \beta^{ex}\left(x; X^0, L^0, k\right)\beta^{in}\left(X^0, 1, L^0, k\right) = \left[(1-k)\left(X^0 - x\right)\right]\left(1 + kX^0 - X^0\right)^{-1}$ (for equilibrium solidification) as it results from eqns (4)-(5).

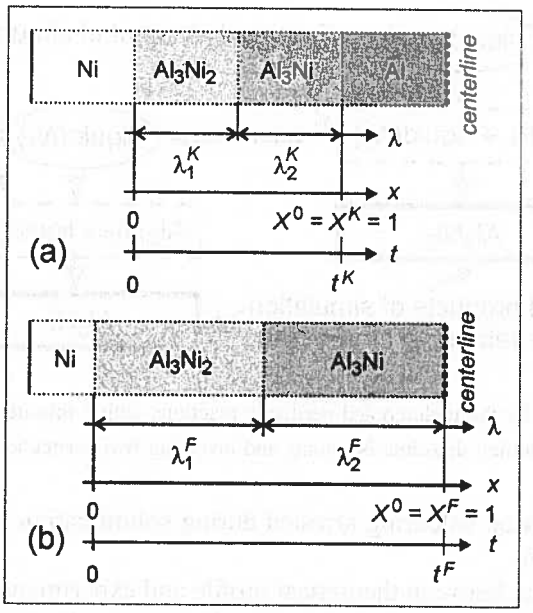

Fig. 10. Sub-layers formed in sequence showing schematically the soldered Ni-Al-Ni multi-layer interconnection; a/ at a given arrested step of formation, b/ just at the disappearance of the Al-liquid filler metal

Acknowledgements

The work has been financially supported by the State Committee for Scientific Research in Poland — the Research Project no 3 T08C 003 27.

REFERENCES

[1] E. Scheil, Zeitschrift für Metallkunde **34**, 70-80 (1942).
[2] H.D. Brody, M. Fleming, Transactions of AIME. **236**, 615-624 (1966).
[3] W. Wołczyński, Back-diffusion phenomenon during the crystal growth by the Bridgman method, Chapter 2 in: Modelling of Transport Phenomena in Crystal Growth, WIT Press 19-59, Southampton, Boston, (2000).
[4] W. Wołczyński, J. Kloch, Bulletin of the Polish Acad. Sci. **46**, 277-300 (1998).
[5] W. Wołczyński, J. Kloch, J. Janczak-Rusch, K. Kurzydłowski, T. Okane, Abstracts of the Fourth International Conference on Solidification and Gravity, 156-157 Miskolc-Lillafüred, (2004).

Received: 10 October 2004.